Semiconductor quantum-wire structures directly grown on high-index surfaces

R. Nötzel, N. N. Ledentsov,* L. Däweritz,† and K. Ploog
Max-Planck-Institut für Festkörperforschung, D-7000 Stuttgart 80, Federal Republic of Germany

M. Hohenstein
Max-Planck-Institut für Metallforschung, D-7000 Stuttgart 80, Federal Republic of Germany
(Received 20 May 1991; revised manuscript received 13 September 1991)

The direct synthesis of GaAs quantum-wire structures on (311)*A* oriented substrates by molecular-beam epitaxy has been achieved due to the *in situ* formation of an array of nanometer-scale macrosteps or facets with a periodicity determined by energy rather than growth-related parameters. These kinds of macrosteps are formed by breaking up a flat surface with high surface energy into facets corresponding to planes with lower surface energy. Reflection high-energy electron diffraction (RHEED) directly reveals the formation of such macrosteps on the GaAs (311)*A* surface comprised of two sets of {331} facets oriented along the [$\bar{2}$33] direction. The lateral periodicity of 32 Å is determined from the splitting of the zeroth-order streak observed along [$\bar{2}$33] into sharp satellites and the height of the steps of 10.2 Å from the splitting along its length. The RHEED intensity dynamics during growth of GaAs/AlAs multilayer structures show a pronounced oscillation at the onset of GaAs and AlAs growth, respectively, due to a phase change of the surface corrugation during the deposition of the first monolayers. The complete structure then contains alternating thicker and thinner channels of GaAs and AlAs forming the quantum wires oriented along [$\bar{2}$33], which is confirmed by high-resolution transmission-electron microscopy. The GaAs quantum-wire structures grown on (311) substrates exhibit a pronounced anisotropy of the electronic properties. Photoluminescence and photoluminescence-excitation (PLE) measurements reveal distinct energy shifts of the excitonic resonances and a strong polarization anisotropy in agreement with theory. Confinement energies up to 90 meV are determined from the appearance of phonon-related lines in the PLE spectra. A strong anisotropy in conductivity is observed in modulation-doped heterostructures. The integrated luminescence intensity of the GaAs quantum-wire structures does not degrade up to temperatures as high as 400 K. This result is important for applications in light-emitting devices.

I. INTRODUCTION

There is currently a strong interest in the investigation of nanometer-scale semiconductor structures having quantum confinement in two[1,2] or three[3] dimensions because of their intriguing physical properties.[4,5] The most important prerequisite for experimental investigations as well as for applications in devices[6,7] is the precise fabrication of nanostructured semiconductors. A widely used method is the patterning of quasi-two-dimensional (2D) heterostructures with nanoscale lithographic techniques.[8] However, the minimum lateral dimensions achieved in such structures are much larger than the vertical dimensions, hence leading to relatively small separations of the subband energies. These small subband spacings are often masked by the level broadening due to fluctuations of the wire width and defects introduced during the patterning process. To reduce especially the defect density, several methods for direct fabrication of quantum-wire structures based on epitaxial growth have been exploited, including growth of tilted superlattices on vicinal substrates,[9,10] growth of grid inserted heterostructures,[11] and strain-induced confinement.[12,13] In these structures, lateral dimensions comparable to the vertical ones can be achieved. They allow in principle for large subband separations, which are required for optical and electrical device applications.[11] The most established method is the growth of tilted superlattices by the deposition of fractional monolayers of alternating composition on stepped surfaces created by a small misorientation from singular surfaces. However, its successful application has so far been very limited due to poor control of local misorientation, kink formation, and stability of the growth rate.[9,10] The produced wires therefore suffer from nonuniformity in shape, dimension, and direction, and up to now no clear manifestation of one-dimensional (1D) confinement effects has been observed.

In this paper we report on a method for the direct synthesis of GaAs quantum-wire structures by molecular-beam epitaxy (MBE). We have developed this method to overcome the present difficulties associated with the direct fabrication.[9,10,14] The basic concept is the *in situ* formation of an array of macrosteps or facets with a periodicity defined by energy rather than growth-related parameters.[15] We show that for conditions typical for the MBE growth process of (Al,Ga)As, i.e., substrate temperature and arsenic pressure, these kinds of macrosteps can be realized on high-index GaAs planes having a high surface energy. A stable configuration is achieved by breaking up the flat surface into facets corresponding to surface planes with lower surface energy. In this way, a continuous formation of well-arranged macrosteps of

 ©1992 The American Physical Society

the desired distance and height is obtained in a reproducible manner. The analysis of reflection high-energy electron diffraction (RHEED) patterns directly shows the existence of such macrosteps on the (311)*A* GaAs surface formed by two sets of {331} facets oriented along the [$\bar{2}$33] direction. The RHEED intensity dynamics during growth of GaAs/AlAs multilayer structures reveal a phase change of the surface corrugation during the deposition of the first monolayers. As additionally confirmed by high-resolution transmission-electron microscopy (HREM), the complete structure then contains alternating thicker and thinner channels of GaAs and AlAs oriented along [$\bar{2}$33] forming the quantum-well-wire superlattice (QWW SL).

The GaAs quantum-wire structures grown on (311) substrates show a pronounced redshift and strong polarization anisotropy of the excitonic transitions in undoped QWW SL's and strong anisotropy of the conductivity in modulation-doped heterostructures. Connected with additional lateral confinement is the appearance of intense phonon related lines in the photoluminescence (PL) and photoluminescence excitation (PLE) spectra and the enhancement of the exciton continuum energies. From the peak energies of the phonon lines in the PLE spectra, the 1D confinement energy is estimated to reach a value as high as 90 meV for a 43-Å GaAs QWW SL. The final striking result is the extremely high integrated luminescence intensity of the new QWW SL, which does not degrade with temperature up to 400 K. This finding is important for applications in light-emitting devices.

This paper is organized as follows. The sample preparation and the experimental setup used for our investigations are described in Sec. II. In Sec. III, the RHEED studies are discussed. Section IV is devoted to the x-ray experiments. In Sec. V we discuss the electronic properties of undoped and modulation-doped GaAs QWW SL's. Finally, in Sec. VI we summarize our results.

II. SAMPLE PREPARATION AND EXPERIMENTAL SETUP

The samples were grown in a RIBER 2300 MBE growth chamber at 600 °C simultaneously on (100) and (311) GaAs substrates, soldered side by side on a molybdenum block. The first series of samples comprised GaAs/AlAs multilayer structures with a total thickness of 0.8 μm and GaAs and AlAs layer thicknesses ranging from 43 to 66 Å in different samples. The second series comprised Si-modulation-doped GaAs/AlAs double heterojunctions with a GaAs layer thickness ranging from 35 to 80 Å in different samples. The growth rate was 1 μm/h for GaAs, and 0.5 μm/h for AlAs, and the As_4/Ga flux ratio was 5. The growth on (311) GaAs was monitored by RHEED using a 30-kV beam from a RIBER CER-1050 electron gun at 1° glancing angle incidence. The measurement system consisted of a video camera, a video recorder, and an image-processing system (VG AUTOLEED).

The structural parameters of the samples were determined with a computer-controlled high-resolution double-crystal x-ray diffractometer in Bragg geometry. A rotating-anode 12-kW generator with a copper target ($\lambda_{CuK\alpha 1}$=0.154 0562 nm) was employed as an x-ray source, and an asymmetrically cut (100) Ge crystal served as monochromator and collimator. The HREM lattice images were taken with a JEOL 4000 FX TEM operating at 400 kV. The PL and PLE measurements were performed with the samples mounted in an optical He-flow cryostat at excitation intensities ranging from 10^{-6} to 50 W cm^{-2}, sample temperatures ranging from 6.5 to 400 K, and different polarizations of the incident light. For luminescence, the red (647.6 nm) and blue (476.2 nm) lines of a Kr^+ laser, and for the PLE measurements, the light from a broadband 600-W halogen lamp dispersed by a 0.5-m double-grating monochromator were used as excitation sources. The luminescence was analyzed by a 1-m single-grating monochromator and detected by a cooled GaAs photomultiplier operating in the photon-counting mode. The conductivity parallel and perpendicular to the surface corrugation was measured at a current of 100 nA and sample temperatures ranging from 4.2 to 300 K. The samples were mesa etched in a geometry of two connected perpendicular hall bars (see inset in Fig. 11), which were carefully aligned parallel and perpendicular to the wires.[16]

III. RHEED STUDIES

After the oxide removal from the GaAs substrate surface at 580 °C in the MBE growth chamber, the RHEED patterns recorded along the [01$\bar{1}$] direction [Fig. 1(a)] and along the [$\bar{2}$33] direction [Fig. 1(b)] directly reveal the breaking up of the flat (311) surface into a well-

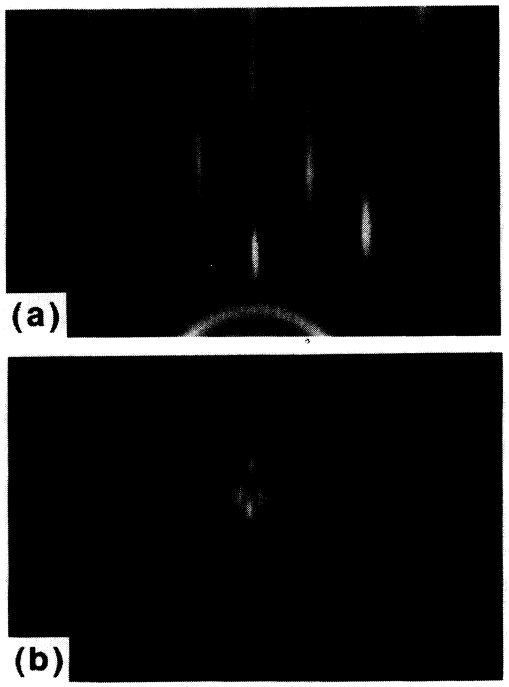

FIG. 1. Reflection high-energy electron-diffraction patterns of the (311) *A* GaAs surface recorded (a) along the [01$\bar{1}$] azimuth and (b) along the [$\bar{2}$33] azimuth.

ordered array of upward and downward steps[17] oriented along the [$\bar{2}33$] direction, as illustrated in Fig. 2(a). With the electron beam along the [$01\bar{1}$] direction, the diffraction pattern [Fig. 1(a)] shows a pronounced streaking, indicating a high density of steps oriented along the perpendicular [$\bar{2}33$] direction. Observing the [$\bar{2}33$] azimuth parallel to the steps, as shown in Fig. 1(b), the streaks are found to be split into sharp satellites or unsplit, depending on the scattering vector $k_\perp$, i.e., the position along the length of the streaks. Furthermore, the intensity maximum of the satellites corresponds to an intensity minimum of the main streak for constant $k_\perp$ values and vice versa. The RHEED pattern recorded in this direction images the reciprocal lattice of the stepped surface,[17] shown in Fig. 2(b). As a consequence, the step height and the periodicity can be determined directly from the separation of the satellites and the splitting along the main streak, respectively. The corresponding intensity profiles measured as a function of $k_\parallel$, i.e., across the streaks for different $k_\perp$ values, and as a function of $k_\perp$ as indicated in Fig. 2(b), are presented in Figs. 3(a)–3(c). The scale is taken from the separation of the zero- and first-order diffraction streaks of the (100) GaAs sample in the [$01\bar{1}$] azimuth. The separation of the satellites in Fig. 3(b) gives the lateral periodicity of 32 Å ($\triangleq 8a_{110}$) for the stepped surface. In this profile, the intensity of the main streak is canceled compared to the intensity of the profile shown in Fig. 3(a) taken at a $k_\perp$ value, where the satellite intensity has a minimum. This intensity distribution evidences the high degree of ordering and the presence of an almost-perfect two-level system.[17] From the splitting of the profile measured along the main streak [Fig. 3(c)], the step height is deduced to be 10.2 Å.

The experimental parameters agree perfectly with our description of the surface [see Fig. 2(a)] to be composed of (311) terraces of 4 Å width ($\triangleq 1a_{110}$) and the two sets of ($33\bar{1}$) and ($\bar{3}1\bar{3}$) facets corresponding to upward and downward steps of 10.2 Å height ($\triangleq 6d_{311}$). In agreement

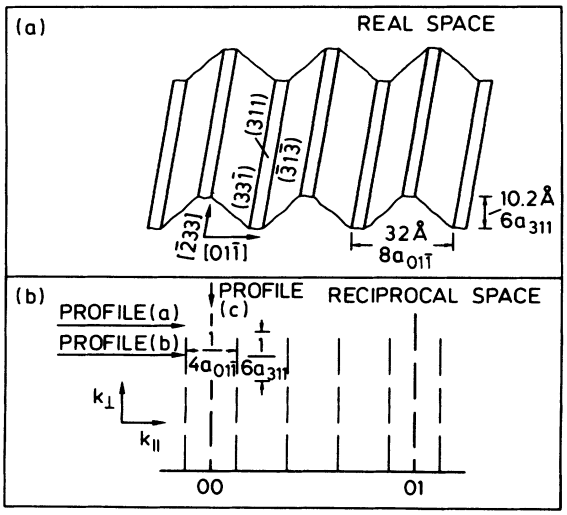

FIG. 2. (a) Schematic of the stepped (311) A GaAs surface. (b) Reciprocal lattice of the stepped surface.

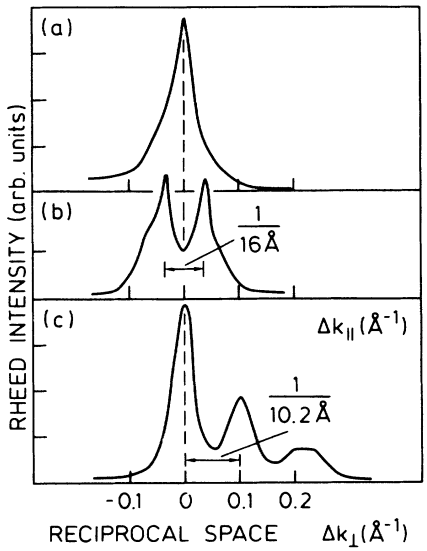

FIG. 3. Reflection high-energy electron-diffraction intensity profiles measured as a function of the scattering vectors $k_\perp$ and $k_\parallel$, respectively, as indicated by arrows in Fig. 2(b).

with surface-energy considerations, the nominal (311) surface breaks up into {331} facets having roughly half the surface energy.[18] The crystallographic model of the stepped surface, including the surface atoms with one or more dangling bonds, is shown in Fig. 4. It clarifies the energetic benefit for the breaking up of the (311) surface in the described manner. It can be seen that the {331} facets are composed of stripes of alternating (110) and (111) surface configurations corresponding to low-index planes with low surface energy.[19] In addition, the specified periodicity and step height leads to a nearly perfect stoichiometry of the stepped surface with an [As]/[Ga] ratio of 13/12.

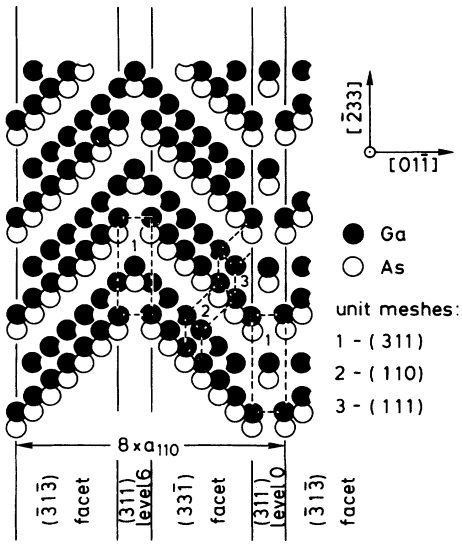

FIG. 4. Crystallographic model of the stepped (311) A GaAs surface including the Ga and As surface atoms with one or more dangling bonds.

The RHEED intensity dynamics inspected along the [$\bar{2}33$] azimuth during the growth of the GaAs/AlAs multilayer structures (Fig. 5) show pronounced oscillations at the onset of GaAs and AlAs growth. As calculated from the respective growth rates, the oscillation corresponds to the deposition of three (311) monolayers, i.e., lattice planes. During the deposition of the next three monolayers, the intensity approaches the value corresponding to the RHEED pattern of the stable stepped surface during growth. The whole sequence corresponds to the deposition of six (311) monolayers, i.e., 10.2 Å, as shown in the inset of Fig. 5 for different growth rates of GaAs and AlAs, and is the consequence of a phase change of the surface corrugation during the heterogeneous deposition of GaAs on AlAs, or vice versa. The phase change, including "quasifilling" of the corrugation during the first three-monolayer deposition and "rearrangement" of the stepped surface during the second three-monolayer deposition, is illustrated by the schematical drawing of the resulting structure in Fig. 5. After the phase change is completed, the growth continues layer by layer with conservation of the surface corrugation, as indicated by the stable RHEED intensity of the stepped surface during growth and by the transition of the RHEED intensity from the nongrowing GaAs (AlAs) surface to the growing GaAs (AlAs) surface within the deposition of one monolayer without any additional structure (shown in the upper curve in Fig. 5 for the growth of GaAs on GaAs).

We assume that the phase change is induced by strain, which plays an important role here and makes the heterogeneous growth on the facets energetically less favorable. Hence, the heterogeneous growth starts on the low-level terrace. However, due to the minimization of the surface energy during the phase change, the atoms will form islandlike channels upon the low-level terrace, having the shape of the corrugated surface, so that the phase change is locally completed. The growth of these islands then causes the observed change in the RHEED intensity, whereby the shape of the RHEED pattern remains unchanged. In this sense, the observed RHEED oscillation has an origin similar to the RHEED oscillations for growth on (100) substrates, which are due to the extension of islands having the height of one monolayer in this case.[20] Consequently, the complete structure consists of well-ordered alternating thicker and thinner regions of GaAs and AlAs oriented along the [$\bar{2}33$] direction, and this unique arrangement indeed forms an as-grown QWW SL's.

This existence of QWW SL's is additionally confirmed by HREM shown in Figs. 6(a) and 6(b) for a sample with average GaAs and AlAs layer thicknesses of 15 Å. The lighter regions are due to AlAs. The cross section is aligned along the [$\bar{2}33$] direction and the projected sample thickness is about 200 Å. The structure is not expected to be imaged with sharp boundaries due to the presence of microroughness of the GaAs/AlAs interface, which extends typically over 1–2 lattice planes, and due to an unintentional 1° slight misorientation of the (311) substrates in a direction 28° off the [$01\bar{1}$] azimuth. However, the average periodicity of 32 Å of the quantum-wire

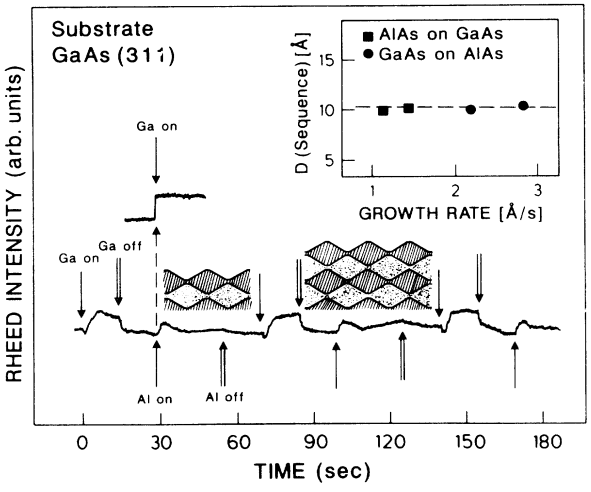

FIG. 5. Reflection high-energy electron-diffraction dynamics measured along the [$\bar{2}33$] azimuth during the growth of GaAs/AlAs multilayer structures on (311) oriented substrates. The upper curve shows the RHEED intensity during the deposition of GaAs on GaAs. In this inset the deposited layer thickness is shown for different growth rates during the growth of GaAs on AlAs and vice versa until stable growth conditions are reached. The schematical drawing images the GaAs/AlAs multilayer structure resulting from the phase change of the surface corrugation during the heterogeneous deposition of the first monolayers of GaAs and AlAs and vice versa.

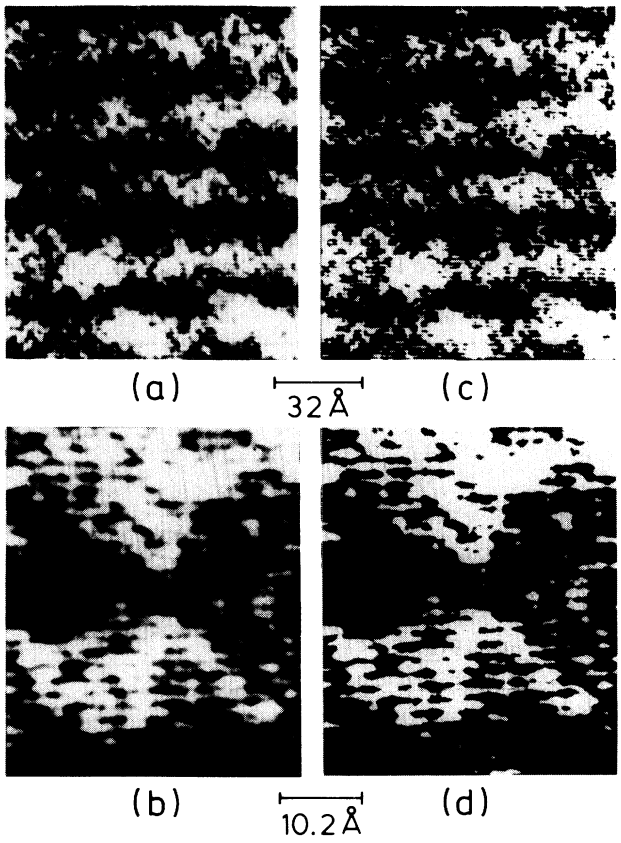

FIG. 6. High-resolution transmission-electron microscopy of a cross section oriented along [$\bar{2}33$]. (a) and (b) show the experimental images, while in (c) and (d) the contrast is enhanced.

array is clearly seen in the experimental image in Fig. 6(a) and in Fig. 6(c) with the contrast enhanced. With higher magnification, the shape of the quantum wire is shown in Figs. 6(b) and 6(d), where the height of the surface corrugation of 10.2 Å and the phase changes of alternating GaAs/AlAs interfaces are obvious.

IV. X-RAY-DIFFRACTION STUDIES

The x-ray-diffraction curves shown in Fig. 7 are recorded in the vicinity of the (311) and (004) reflections of the (311) and (100) oriented GaAs/AlAs multilayer structures, respectively. The structural perfection is comparable for both samples, as can be seen from the width and intensity of the diffraction peaks.[21] The average Al concentration x is determined from the angular spacing between the substrate peak and the epitaxial layer peak (zeroth-order peak) by applying Vegard's rule with $x = \Delta\Theta/\Delta\Theta_{AlAs}$, where $\Delta\Theta_{AlAs}$ is the angular spacing for the GaAs/AlAs system. The value of $\Delta\Theta_{AlAs}$ is independently determined for the [311] and [100] growth directions from 3000-Å-thick AlAs epilayers grown on (311) and (100) GaAs substrates as reference to be 1.25 and 1.81 mrad, respectively. Finally, the angular distance between the zeroth-order peak and the satellite peaks yields for the samples presented here 56 Å for the GaAs layer thickness of the (100) sample and also 56 Å for the average GaAs layer thickness of the (311) sample. In the same manner, the AlAs layer thicknesses are found to be 50 Å for both orientations.

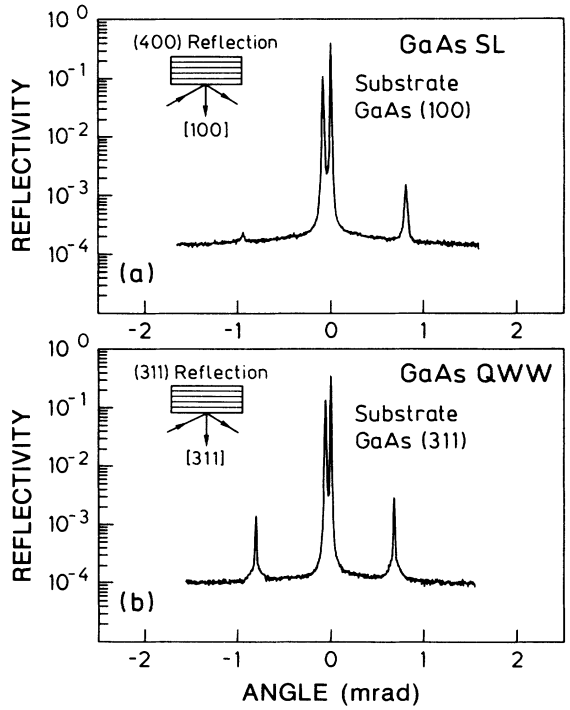

FIG. 7. Double-crystal x-ray-diffraction patterns in the vicinity of the symmetrical reflections of (a) (100) and (b) (311) oriented GaAs/AlAs multilayer structures.

V. ELECTRONIC PROPERTIES

A. Optical properties

The GaAs QWW SL's directly grown on the (311) substrate show a clear polarization anisotropy of the excitonic resonances.[22–25] In the present structure, where strong coupling between the quantum wires has to be assumed, this optical anisotropy, originating from lateral confinement due to the strong periodic lateral potential[25] that is introduced by the presence of alternating thicker and thinner GaAs and AlAs regions, is reduced relative to the isolated wire case.[23] The PL, PLE, and the photoluminescence suppression (PLS) spectra of the GaAs buffer layer luminescence are shown in Figs. 8(a)–8(c) for a 66-Å GaAs QWW SL. The narrow linewidth of 5 meV of the PL line shown in Fig. 8(a) reflects the high structural perfection of the QWW SL. The PLE spectra shown in Fig. 8(b) clearly evidence the lateral confinement. With the light polarized parallel to the wires, the heavy-hole resonance is more pronounced compared to the case with the light polarized perpendicular to the wires, where the light-hole resonance is more in-

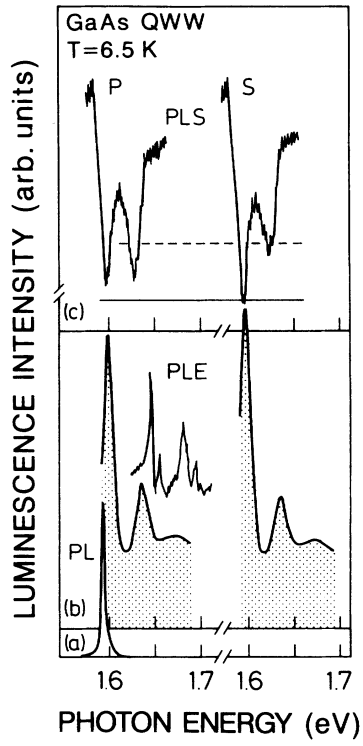

FIG. 8. (a) Photoluminescence (PL), (b) photoluminescence excitation (PLE), and (c) photoluminescence suppression (PLS) spectra of the GaAs quantum-well-wire (QWW) superlattice with a GaAs layer thickness of 66 Å and an AlAs layer thickness of 60 Å. The sample temperature is 6.5 K. The excitation intensity is 10^{-6} W cm^{-2} for (b) and (c) and 50 W cm^{-2} for (a) with the wavelength of 647.6 nm. P corresponds to light polarized perpendicular to the wire axis, and S to light polarized parallel to the wire axis. The additional lines in (b) are detected on the high-energy side of the PL line and correspond to LO and TA phonon related lines.

tense. The optical anisotropy is further demonstrated in the PLS spectra shown in Fig. 8(c). By detecting the luminescence of the GaAs buffer layer, this method measures directly the absorption of the QWW SL, and hence the intrinsic polarization anisotropy of the excitonic transition of the present structure can be determined accurately. The observed optical anisotropy is of the order of 15% for the heavy-hole exciton resonance and 30% for the light-hole exciton resonance. This magnitude of the optical anisotropy is quite realistic for the present structure, where the finite barrier heights, significant coupling between the quantum wires, and their sophisticated shape have to be considered.[25] In addition, the corresponding polarization anisotropy exists in the room-temperature luminescence of the QWW SL, where the free-electron–heavy-hole and electron–light-hole transitions are observed. It should be noted here that for the (100) SL reference sample grown side by side, and also for the luminescence of the GaAs buffer layer of the QWW SL, no polarization dependence is observed.

To complete the picture the in-plane luminescence from the cleavage planes is investigated for the reference SL and the QWW SL. As expected, the in-plane luminescence of the SL is polarized perpendicular to the z (growth) direction,[26,27] whereas the in-plane luminescence of the QWW SL shows a pronounced component that is polarized parallel to the z direction. This component of the luminescence is even more pronounced for the case of the quantum wires aligned perpendicular to the cleavage plane, as compared to the case where the alignment is parallel to this plane. This behavior again demonstrates the influence of the additional lateral confinement on the optical anisotropy and shows that efficient quantization is also relevant for a direction perpendicular to the z direction.

If the detection wavelength is set to the high-energy side of the luminescence line, sharp lines in the low-excitation intensity (10^{-6} W cm^{-2}) PLE spectra of the QWW SL are resolved [Fig. 8(b)]. The peak energies are separated by 36 and 12 meV, and hence the lines correspond to LO and TA phonon related lines. The PLE spectra of the reference SL show only one very weak LO phonon line. The appearance of these strong phonon related lines in the QWW SL is thus connected with the additional lateral confinement. It is unlikely that their origin is due to Raman scattering rather than to hot excitons, since the lines do not maintain circular and linear polarization, and they broaden up to 10 meV if the detection wavelength is set to lower energies. On the other hand, a distinction between resonant Raman-scattering and hot-exciton luminescence is meaningless when their respective relevant time scales, i.e., the exciton dephasing time and the exciton lifetime, are similar.[28,29]

We ascribe the lines as being due to indirect creation and relaxation of strongly laterally localized hot excitons created in the 1D continuum. In general, the occurrence of phonon related lines is indicative for excitons in materials with strong exciton-phonon coupling, increased exciton binding energies, or efficient exciton localization.[30] Recently, the enhancement of phonon replica of localized exciton emission was reported for direct-band-gap quantum wells in high magnetic fields and attributed to the magnetic-field-induced lateral localization of excitons.[31] In our GaAs QWW SL, both the additional lateral exciton confinement and the resulting increase of the quasi-1D continuum energies for heavy holes and light holes are responsible for this behavior. The 1D continuum energies for heavy holes and light holes are estimated from additional features in the PLE spectra of a 56-Å QWW SL observed 19 and 26 meV above the heavy-hole and light-hole excitonic resonances, respectively. For the (100) reference sample, the respective 2D continuum energies are observed 8 and 10 meV above the heavy-hole and light-hole exciton resonances, in agreement with excitonic binding energies in quantum wells.[32] For the 66-Å GaAs QWW SL shown in Fig. 8, the 1D continuum energy for the light hole corresponds to the additional feature observed in PLE above the light-hole exciton transition.

The additional confinement in the QWW SL leads to an increased probability for the excitons created in the 1D continuum to relax and recombine as a whole,[33] and hence increased interaction of phonons with the excitons is observed. For excitation energies in the 2D continuum, which correspond to transition energies in the thinner GaAs regions, however, strong damping of the phonon lines is expected. It is important to note that this energy threshold provides an estimate of the 1D confinement energy. We have observed the described behavior for different QWW SL samples with GaAs layer thicknesses of 66, 56, and 43 Å. In the case of the 66-Å QWW SL shown in Fig. 8(b), damping exists already for the second LO phonon line. However, for the 56- and 43-Å GaAs QWW SL's, the phonon lines are observed with equal intensities up to the 2LO+TA phonon line, whereas the following phonon lines are strongly damped. The appearance of undamped phonon lines up to higher energies for decreasing GaAs layer thickness reflects the corresponding increase of the 1D confinement energy. The striking result is that the 1D exciton confinement energy ($E_{\mathrm{SL}}-E_{\mathrm{QWW\,SL}}$), estimated from this behavior, reaches values up to 90 meV for the 43-Å GaAs QWW SL. The increased interaction with phonons can be observed also on the low-energy side of the luminescence spectra of the QWW SL's at low temperatures, where in contrast to the reference SL, the LO phonon replica are found to be strongly enhanced.

Although of the same average layer thicknesses, the luminescence line of the QWW SL is shifted to *lower* energies compared to the (100) reference sample grown side by side. This redshift is due to the fact that the luminescence of the QWW SL originates from transitions in the *thicker* GaAs quantum-wire regions. The redshift increases from 3–5 meV for the 66-Å sample to 24 meV for the 43-Å GaAs sample, as is shown in Figs. 9(a)–9(d) for the corresponding PL spectra at 300 K. This variation reflects the increased influence of the interface corrugation for decreased GaAs layer thickness.

The QWW SL's in general exhibit an extremely high integrated luminescence intensity that is comparable to the (100) reference sample at 6.5 K. Even at moderate excitation densities of the order of 10 W cm^{-2}, unit quan-

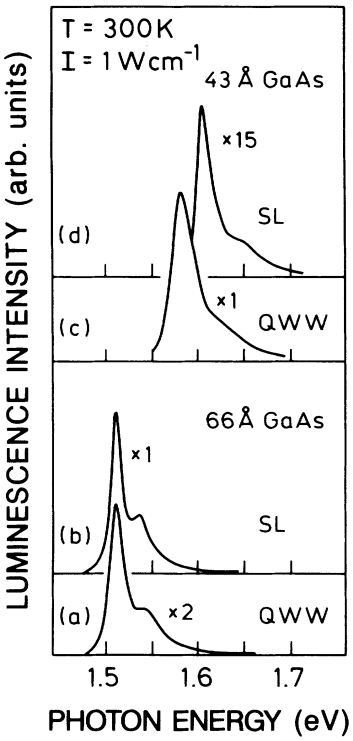

FIG. 9. Room-temperature luminescence of (a) a 66-Å GaAs quantum-well-wire superlattice (QWW), (b) a 66-Å GaAs superlattice (SL), (c) a 43-Å GaAs QWW SL, and (d) a 43-Å GaAs SL. The excitation wavelength is 647.6 nm.

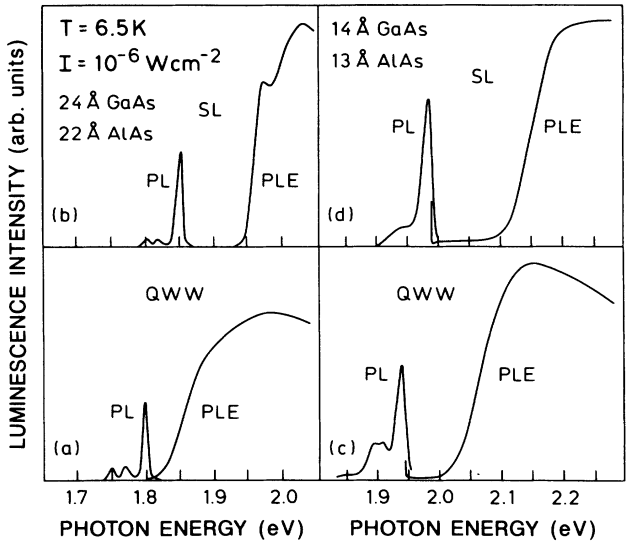

FIG. 10. Photoluminescence PL and PL excitation (PLE) spectra of (a) a 24-Å GaAs, 22-Å AlAs short-period quantum-well-wire superlattice (SP QWW SL), (b) a 24-Å GaAs, 22-Å AlAs SP SL, (c) a 14-Å GaAs, 13-Å AlAs SP QWW SL, and (d) a 14-Å GaAs, 13-Å AlAs SP SL. The excitation wavelength for the PL spectra is 600 nm.

tum efficiency is achieved. At room temperature, however, the integrated luminescence intensity of the 66-Å GaAs QWW SL is comparable to that of the reference SL sample [see Figs. 9(a) and 9(b)], whereby for the 43-Å GaAs QWW SL the integrated luminescence intensity is more than one order of magnitude higher than that of the reference SL sample [see Figs. 9(c) and 9(d)], and does not degrade up to 400 K. This behavior again arises from the additional lateral confinement of the present structure. The nonradiative interface recombination is in this case strongly suppressed due to the reduced spreading of the carriers, which is now freely possible only in the direction parallel to the wires. To achieve the desired localization of the carriers at room temperature, however, the average GaAs layer thickness has to be thinner than 66 Å, which is in agreement with the estimate of the 1D confinement energy given before. This finding is important for the design of light-emitting devices of high efficiency at room temperature.

As a final point regarding the optical properties, we briefly outline some interesting phenomena concerning short-period (SP) QWW SL's. The SP QWW and the reference SP SL's become indirect for GaAs and AlAs layer thicknesses below 35 Å. The PL spectra shown in Figs. 10(a) and 10(b) reveal a strong zero phonon line and weak phonon sidebands and are typical for the conduction-band minimum to be at the X_z point in the AlAs layers.[34–36] Although the SP QWW SL's are of high structural perfection, the PLE spectra [Fig. 10(a)] reveal a smooth onset and a pronounced overlap with the PL line. This behavior shows a strong mixing between the Γ and the X_z minima, which is assumed to be due to the interface corrugation. In contrast, the PLE spectra of the SP SL [Fig. 10(b)] show a sharp onset well separated from the PL line. The strong $\Gamma - X_z$ mixing, even for type-II SP QWW SL's with high-energy separation between the Γ and X minima, results in an integrated luminescence intensity that does not degrade significantly up to room temperature. This finding offers the possibility of fabricating optical devices that work with high efficiency at energies even above the limit for direct-gap $GaAs/Al_xGa_{1-x}As$ SL's.

For SP QWW SL's with layer thicknesses below 20 Å, the phonon sidebands in the PL spectra are drastically increased with respect to the zero phonon line compared to the reference SP SL [see Figs. 10(c) and 10(d)]. Mixing is absent in this case. With a temperature rise, the whole PL spectrum of the reference SP SL drops very rapidly in intensity, which is typical for X type-II SP SL's, whereas for the SP QWW SL, only the zero phonon line drops rapidly, and the spectrum is dominated by the phonon sidebands up to high temperatures. A similar behavior was recently reported for ultra SP SL's, where also the L minimum in the GaAs layers is determined to be the lowest one in the conduction band.[37]

B. Electrical measurements

Additional confirmation of the 1D character of the present QWW SL structure is obtained from the anisotropy of the conductivity of Si- (p-type[38]) modulation-doped GaAs quantum wires. The samples are mesa etched in an L-shaped geometry shown in the inset of Fig. 11. The four terminal conductivities perpendicular and parallel to the quantum wires are measured at a current of $I = 100$

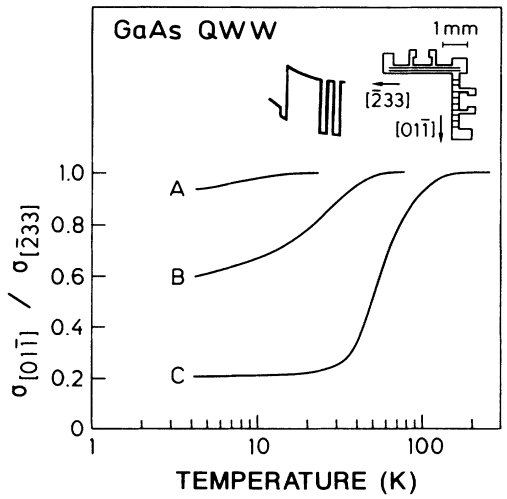

FIG. 11. Anisotropy of the conductivity of p-type modulation-doped quantum wires with average GaAs layer thicknesses of (A) 80 Å, (B) 50 Å, and (C) 35 Å measured at a current of $I=100$ nA. The geometry of the mesa etched structures and the schematic of the energy band structure are shown in the inset.

nA. The ratio of the conductivities perpendicular and parallel to the quantum wires as a function of the sample temperature is shown in Fig. 11. The curves correspond to different samples with average GaAs layer thicknesses of 80, 50, and 35 Å. The average density of holes per unit area deduced from Hall measurements amounts to 2×10^{11} cm^{-2} for the investigated samples. For the 80-Å GaAs quantum wire we observe almost no anisotropic behavior. However, the anisotropy of the conductivity is increased from 1.6 for the 50-Å GaAs quantum wire to 4.6 for the 35-Å GaAs quantum wire at low temperature, whereby the observed onset of the anisotropy moves to higher temperatures. Since for the present carrier concentrations the wave vector of the lateral potential modulation $\pi/32$ Å exceeds the Fermi wave vector by one order of magnitude, the dispersion relation of the holes is not expected to be altered drastically as in the case of planar superlattices.[39,40] Additionally, for the 50- and 35-Å GaAs samples, the Fermi energy is below the 1D confinement energy for holes estimated from the optical investigations. Therefore, we assume that the anisotropy of the conductivity in the present structures originates mainly from the lateral confinement of the holes, which is expected to be significant in the quantum wires.[25] From the observed onset of the anisotropy as a function of the temperature, the 1D confinement energies for the holes can be estimated very roughly to be 8 meV for the 35-Å GaAs quantum wire and 3 meV for the 50-Å GaAs quantum wire. These values are quite close to the values estimated for the 1D confinement energies for the holes from our optical investigations. In this sense, the electrical measurements complete the picture that has been derived from the optical investigations.

VI. CONCLUSION

In summary, we have developed a method for the direct synthesis of semiconductor quantum-wire structures on high-index substrates. Due to its high surface energy, the (311) surface breaks up into regular facets having nanometer scale dimensions, which is directly monitored by RHEED. In addition, RHEED dynamics evidences a unique growth mechanism on the stepped surface. Thicker and thinner regions of GaAs and AlAs are built up regularly, thus forming the QWW SL. The 1D character of the QWW SL is reflected in a polarization anisotropy of the excitonic transitions and in a strong anisotropy of the conductivity in modulation-doped quantum wires. Confinement energies up to 90 meV are estimated from the appearance of LO and TA phonon lines in the PLE spectra. A pronounced Γ-X mixing is observed for type-II SP QWW SL's. The extremely high integrated luminescence intensity of the QWW SL does not degrade up to 400 K, which shows high structural perfection and makes the new QWW SL important for applications in quantum-wire lasers.

ACKNOWLEDGMENTS

The authors would like to thank A. D. Wieck and V. F. Sapega for many useful discussions, and H. Lage for a critical reading of the manuscript.

*On leave from A. F. Ioffe Physico Technical-Institute, Leningrad, U.S.S.R.
†On leave from Zentralinstitut für Elektronenphysik, Berlin, FRG.

[1]J. S. Weiner, G. Danan, A. Pinczuk, J. Valladares, L. N. Pfeiffer, and K. West, Phys. Rev. Lett. **63**, 1641 (1989).
[2]J. M. Hong, T. P. Smith, K. Y. Lee, C. M. Knoedler, S. E. Laux, D. P. Kern, and L. Esaki, J. Cryst. Growth **95**, 266 (1989).
[3]M. A. Reed, J. N. Randall, R. J. Aggarwal, R. J. Matyi, T. M. Moore, and A. E. Wetsel, Phys. Rev. Lett. **60**, 535 (1988).
[4]H. Sakaki, Jpn. J. Appl. Phys. **19**, L735 (1980).
[5]M. L. Roukes, A. Scherer, S. J. Allen, H. G. Craighead, R. M. Ruthen, E. D. Beebe, and J. P. Harbison, Phys. Rev. Lett. **59**, 3011 (1987).
[6]Y. Arakawa and H. Sakaki, Appl. Phys. Lett. **40**, 939 (1982).
[7]E. Kapon, D. Hwang, and R. Bhat, Phys. Rev. Lett. **63**, 430 (1989).
[8]M. Kohl, D. Heitmann, P. Grambow, and K. Ploog, Phys. Rev. Lett. **63**, 2124 (1989).
[9]M. Tsuchiya, J. M. Gaines, R. H. Yan, R. J. Simes, P. O. Holtz, L. A. Coldren, and P. M. Petroff, Phys. Rev. Lett. **62**, 466 (1989).
[10]T. Fukui and H. Saito, Jpn. J. Appl. Phys. **29**, L731 (1990).
[11]M. Tanaka, J. Motohisa, and H. Sakaki, Surf. Sci. **228**, 408 (1990).
[12]D. Gershoni, J. S. Weiner, S. N. Chu, G. A. Baraff, J. M. Vandenberg, L. N. Pfeiffer, K. West, R. A. Logan, and T. Tanbun-Ek, Phys. Rev. Lett. **65**, 1631 (1990).
[13]K. Kash, B. P. v. d. Gaag, J. M. Worlock, A. S. Gozdz, D. D.

Mahoney, J. P. Harbison, and L. T. Florez, in *Localization and Confinement of Electrons in Semiconductors,* edited by F. Kuchar, H. Heinrich and G. Bauer, Springer Series in Solid-State Sciences Vol. 97 (Springer-Verlag, Berlin, 1990), p. 39.

[14]E. Corcoran, Sci. Am. **263**, 74 (1990).

[15]E. L. Williams and N. C. Bartelt, Science **251**, 393 (1991).

[16]D. Weiss, in *Localization and Confinement of Electrons in Semiconductors* (Ref. 13), p. 247.

[17]M. G. Lagally, D. E. Savage, and M. C. Tringides, in *Reflection High-Energy Electron Diffraction and Reflecting Electron Imaging of Surfaces,* Vol. 188 of *NATO Advanced Study Institute, Series B: Physics,* edited by P. K. Larsen and P. J. Dobson (Plenum, New York, 1988), p. 139.

[18]D. J. Chadi, Phys. Rev. B **29**, 785 (1984).

[19]C. Messmer and J. C. Bilello, J. Appl. Phys. **52**, 4623 (1981).

[20]J. H. Neave, B. A. Joyce, P. J. Dobson, and N. Norton, Appl. Phys. A **31**, 1 (1983).

[21]L. Tapfer and K. Ploog, Phys. Rev. B **33**, 5565 (1986).

[22]E. Kane, J. Chem. Solids **1**, 249 (1957).

[23]P. C. Sercel and K. J. Vahala, Appl. Phys. Lett. **57**, 545 (1990).

[24]U. Bockelmann and G. Bastard, Europhys. Lett. **15**, 215 (1991).

[25]D. S. Citrin and Y. C. Chang, Phys. Rev. B **43**, 11 703 (1991).

[26]C. Weisbuch, in *Physics and Applications of Quantum Wells and Superlattices,* edited by E. E. Mendez and K. v. Klitzing (Plenum, New York, 1987), p. 261.

[27]J. S. Weiner, D. S. Chemla, D. A. B. Miller, H. A. Haus, A. C. Gossard, W. Wiegmann, and C. A. Burns, Appl. Phys. Lett. **47**, 664 (1985).

[28]R. P. Stanley, J. Hegarty, R. Fischer, J. Feldmann, E. O. Göbel, R. D. Feldman, and R. F. Austin, Phys. Rev. Lett. **67**, 128 (1991).

[29]M. V. Klein, Phys. Rev. B **8**, 919 (1973).

[30]S. Permogorov, Phys. Status Solidi B **68**, 9 (1975).

[31]K. J. Nash, M. S Skolnick, P. A. Claxton, and J. S. Roberts, Phys. Rev. B **39**, 5558 (1989).

[32]R. C. Miller and D. A. Kleinman, J. Lumin. **30**, 520 (1985).

[33]P. S. Kop'ev, D N. Mirlin, V. F. Sapega, and A. A. Sirenko, Pis'ma Zh. Eksp. Teor. Fiz. **51**, 624 (1990) [JETP Lett. **51**, 708 (1990)].

[34]R. Cingolani, L. Baldassarre, M. Ferrara, M. Lugara, and K. Ploog, Phys. Rev. B **40**, 6101 (1989).

[35]H. W. v. Kesteren, E. C. Cosman, P. Dawson, K. J. Moore, and C. T. Foxon, Phys. Rev. B **39**, 13 426 (1989).

[36]R. Cingolani, K. Ploog, L. Baldassarre, M. Ferrara, M. Lugara, and C. Moro, Appl. Phys. A **50**, 189 (1990).

[37]M. D. Sturge, F. E. Weikun, W. S. Schmidt, L. N. Pfeiffer, and K. West, in *Proceedings of the 20th International Conference on the Physics of Semiconductors,* edited by E. M. Anastassakis and J. D. Joannopoulos (World Scientific, Singapore, 1990), Vol. 2, p. 1029.

[38]W. I. Wang, E. E. Mendez, T. S. Kuan, and L. Esaki, Appl. Phys. Lett. **47**, 826 (1985).

[39]J. Motohisa, M. Tanaka, and H. Sakaki, Appl. Phys. Lett. **55**, 1214 (1989).

[40]K. Ensslin, S. A. Chalmers, P. M. Petroff, A. C. Gossard, and H. Kroemer, Superlatt. Microstruct. **9**, 119 (1991).

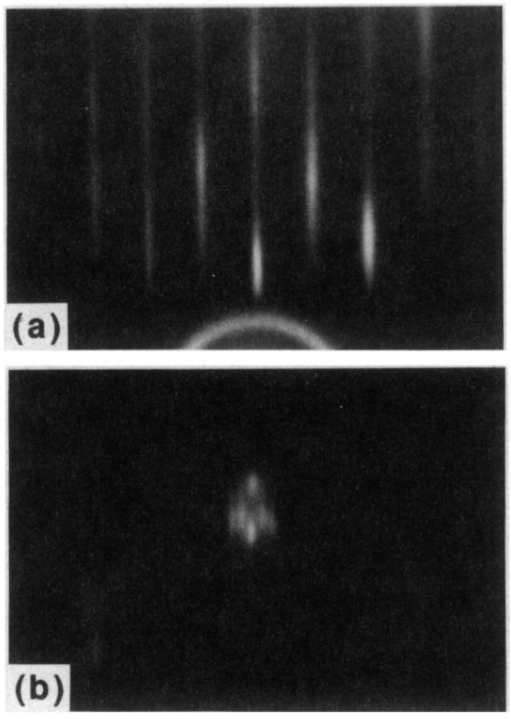

FIG. 1. Reflection high-energy electron-diffraction patterns of the (311) *A* GaAs surface recorded (a) along the $[01\bar{1}]$ azimuth and (b) along the $[\bar{2}33]$ azimuth.

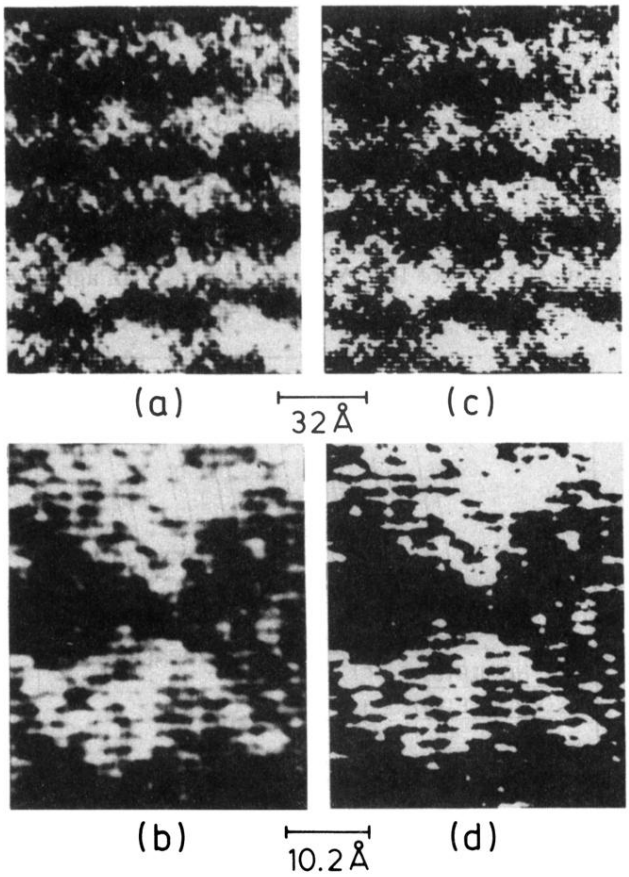

FIG. 6. High-resolution transmission-electron microscopy of a cross section oriented along [$\bar{2}33$]. (a) and (b) show the experimental images, while in (c) and (d) the contrast is enhanced.